Aust. J. Phys., 1980, 33, 261–81

Relativistic Effects in Electron Scattering by Atoms. I Elastic Scattering by Mercury

L. T. Sin Fai Lam

Electron and Ion Diffusion Unit, Research School of Physical Sciences,
Australian National University, P.O. Box 4, Canberra, A.C.T. 2600.

Abstract

Elastic scattering of electrons in the energy range 0–25 eV by mercury atoms is investigated by applying a perturbation method to the (nonrelativistic) Schrödinger equation. Relativistic correction to the potential is treated using two models: a Pauli approximation and a second-order Dirac potential. The nonrelativistic Hartree–Fock wavefunction is used to describe the target in the zeroth order approximation. Electron exchange is found to be important in the collision. The relativistic correction due to mass variation makes a significant contribution, in particular to p-wave scattering which is dominated by a low energy shape resonance. Phase shifts for s-, p-, d- and f-wave scattering are presented. An analytic expression for the momentum transfer cross section for relativistic scattering is obtained. The total cross section, momentum transfer cross section, differential cross section and spin polarization are calculated and compared with experiment.

Introduction

Relativistic effects in the structures of heavy atoms can be studied by using two different theoretical approaches:

(i) By taking explicit account of relativistic corrections in the calculation of wavefunctions by the use of the Dirac equation (Swirles 1935; Grant 1961). The calculations can become quite complicated and have been done only for fairly simple systems (Coulthard 1967; Kim 1967; Desclaux *et al.* 1971).

(ii) By applying perturbation theory to the low-Z Pauli Hamiltonian to calculate relativistic corrections using basis set wavefunctions which give a good solution of the nonrelativistic problem. In this method the relativistic terms of the Hamiltonian are considered to be small in comparison with the leading nonrelativistic operators (Bethe and Salpeter 1957). The method is much easier to use than (i) above and extensive calculations have been made on the structures of ions and atoms (e.g. Blume and Watson 1962, 1963, 1964; Herman and Skillman 1963; Malli 1967; Beck 1969; Jones 1970).

The collisions between electrons and heavy atoms can also be treated using these two different methods. Earlier calculations based on the Dirac equation have used a strongly screened Coulomb field with electron exchange neglected (Bunyan 1963; Holzwarth and Meister 1964; Bühring 1968; Weiss 1969). Carse and Walker (1973) have used the Dirac equation to formulate a theory of electron–atom scattering, and Walker (1969, 1970*a*, 1970*b*, 1971, 1975) has made calculations for several atoms with nuclear charge Z in the range $2 \leqslant Z \leqslant 100$. The work of Walker gives considerable insight into the nature of relativistic effects in scattering problems.

However, since the Dirac equation is used, the various relativistic effects cannot be separated and their relative contributions are difficult to assess.

The method (ii) above has been used by Norcross (1973) to study the photo-ionization of caesium, and by Burke and Mitchell (1974) to treat the electron–caesium collision. However, the relativistic correction due to spin–orbit interaction only was taken into account in these calculations. Browne and Bauer (1966) have also used a perturbation method with the second-order Dirac potential, which takes higher order relativistic effects into account, but they did not consider exchange in the calculation. A formulation of the scattering problem based on the Breit–Pauli approximation, with higher order relativistic corrections taken into account, has been developed by Jones (1975) using the variational principle.

Another theoretical approach is phase shift analysis, which has been extended by Hutt and Bransden (1974) and Hutt (1975) to treat the elastic scattering of electrons by mercury atoms at low energies. The method has been used with success to analyse the electron–helium system for which there is an adequate experimental data set (Bransden 1976). However, it has been more difficult to apply it to the electron–mercury system because of insufficient data until recently. Moreover, for this system there are, for every partial wave $l > 0$, two phase shifts corresponding to spin up and spin down.

In this work we consider the elastic scattering of low energy electrons by a closed shell heavy atom. The electron–mercury system has been chosen to test the theoretical approach here since, in addition to relativistic calculations by Walker (1969, 1970*a*, 1970*b*, 1975, personal communication), there is a wealth of recent experimental data for comparison. Data on the total cross section are available from a beam experiment (Jost and Ohnemus 1979), the momentum transfer cross section from a swarm experiment (Elford 1980; present issue, pp. 251–9) and the differential cross section and spin polarization from double scattering experiments (Deichsel *et al.* 1966; Eitel *et al.* 1968; Eitel and Kessler 1970; Duweka *et al.* 1976). A survey of earlier experiments and calculations has been given by Kessler (1969).

We choose a perturbation technique to investigate relativistic effects using two methods based on (1) the Pauli approximation and (2) the second-order Dirac potential. The importance of exchange is examined. The relativistic correction due to mass variation is found to make a significant contribution. The results indicate that p-wave scattering is dominated at low energy by a shape resonance, in agreement with experiment. Spin–orbit interaction splits this structure into two resonance peaks: a broad one for the $p_{3/2}$ and a sharper one for the $p_{1/2}$ partial wave phase shifts. An analytic expression for the momentum transfer cross section in the relativistic case is derived. Finally, we compare theory with experiment for the total cross section, momentum transfer cross section, differential cross section and spin polarization.

Theory

Consider the collision of an electron with an N-electron atom. The total wave-function of the system can be written as

$$\Psi(1,2,...,N+1) = (N+1)^{-\frac{1}{2}} \sum_{i=1}^{N+1} (-)^{N+1-i}\psi(1,2,...,i-1,i+1,...,N+1)\,F^{p}(i), \quad (1)$$

where $\boldsymbol{i}$ denotes the space and spin coordinates of the ith electron, ψ is the target function

$$\psi = N^{-\frac{1}{2}} \varepsilon_{\alpha_i,\beta_i,\ldots,\pi_i\ldots} \phi_{\alpha_i}(1)\,\phi_{\beta_i}(2)\ldots\phi_{\pi_i}(N)\ldots \tag{2}$$

and F^p is the continuum function which describes the motion of the scattered electron. Using the j–j coupling representation, we write the orbital ϕ for an electron with quantum numbers (n, κ, μ) and the continuum function F^p as

$$\phi(\boldsymbol{i}) = R_{n\kappa}(r)\,\chi_{\kappa,\mu}(\hat{r}), \qquad F^p(\boldsymbol{i}) = F_\kappa(r)\,\chi_{\kappa,\mu}(\hat{r}), \tag{3a, b}$$

where the angular functions are given by

$$\chi_{\kappa,\mu}(\hat{r}) = \sum_{m_l} \mathrm{C}^{l\ s\ j}_{m_l m_s \mu}\, \mathrm{Y}_{l,m_l}(\hat{r})\, \sigma_{s,m_s}. \tag{4}$$

The symbol κ gives both the total angular momentum j and the orbital angular momentum l of the electron according to

$$j = |\kappa| - \tfrac{1}{2}, \tag{5}$$

$$l = \kappa \qquad \text{for} \qquad \kappa > 0, \tag{6a}$$

$$= -\kappa - 1 \qquad\qquad \kappa < 0. \tag{6b}$$

In equation (4) $\mathrm{C}^{l\ s\ j}_{m_l m_s \mu}$ is the Clebsch–Gordan coefficient, $\mathrm{Y}_{l,m_l}(\hat{r})$ is the normalized spherical harmonic and σ_{s,m_s} is the usual two-component spinor. Note that the relativistic wavefunction, obtained by solution of the Dirac equation, is an antisymmetrized combination of one-electron orbitals defined as

$$\phi_{n\kappa\mu}(\boldsymbol{r}) = \begin{pmatrix} r^{-1} P_{n\kappa}(r)\,\chi_{\kappa\mu}(\hat{r}) \\ \mathrm{i}r^{-1} Q_{n\kappa}(r)\,\chi_{-\kappa\mu}(\hat{r}) \end{pmatrix}, \tag{7}$$

where $r^{-1} P_{n\kappa}(r)$ and $r^{-1} Q_{n\kappa}(r)$ are the large and small radial wavefunctions respectively, which satisfy the orthogonality condition

$$\int_0^\infty \mathrm{d}r\,\{P_{n\kappa}(r)\,P_{n'\kappa}(r) + Q_{n\kappa}(r)\,Q_{n'\kappa}(r)\} = \delta_{nn'}. \tag{8}$$

The radial part $R_{n\kappa}(r)$ of equation (3a) is equivalent to $r^{-1} P_{n\kappa}(r)$ of equation (7), if the small component $r^{-1} Q_{n\kappa}(r)$ is assumed to be negligible.

The Hamiltonian of the $(N+1)$-electron system is written as

$$H_{N+1} = \sum_{i=1}^{N+1} (-\tfrac{1}{2}\nabla_i^2 - Z/r_i) + \sum_{i>j=1}^{N+1} |\boldsymbol{r}_i - \boldsymbol{r}_j|^{-1} + h_r. \tag{9}$$

The first two terms on the right-hand side of this equation comprise the nonrelativistic Hamiltonian while h_r is the relativistic correction to the potential. In the present calculation we consider only the ground state of the target. Nonrelativistic HF wavefunctions (Froese-Fischer 1972) are used in equation (2) and relativistic corrections to the potential of the target electrons are not taken into account in equation (9). The term h_r describes the relativistic correction to the interaction between the scattered electron and the target atom. It is treated as a first-order perturbation to the Hamiltonian. Two types of potential are used for h_r, and we now consider these models,

(1) *Pauli Approximation*

In this model the relativistic correction to the potential is written as a sum of one- and two-particle contributions to the Hamiltonian (Bethe and Salpeter 1957; Jones 1975). One-body operators make the largest contribution to the relativistic corrections and their contribution relative to that of two-body operators increases with the nuclear charge (Beck 1969; Jones 1970). Neglecting two-body operators and higher order terms, we write

$$h_r = f(\mathrm{M}) + f(\mathrm{D}) + f(\mathrm{SO}), \tag{10}$$

where

$$f(\mathrm{M}) = -\tfrac{1}{8}\alpha^2\nabla^4, \qquad f(\mathrm{D}) = -\tfrac{1}{8}Z\alpha^2\nabla^2(r^{-1}), \qquad f(\mathrm{SO}) = \zeta(r)\boldsymbol{l}.\boldsymbol{s}, \tag{11}$$

with the Sommerfeld fine-structure constant $\alpha = 1/137{\cdot}037$. Here $f(\mathrm{M})$ accounts for the variation of electron mass with velocity, $f(\mathrm{D})$ is a relativistic correction to the potential (which has no classical analogue and is sometimes called the Darwin operator) and $f(\mathrm{SO})$ describes the spin–orbit effect using a suitable choice for the radial function $\zeta(r)$ to give the dominant contribution to the one-particle magnetic interaction.

The equation for the continuum function can be derived by applying the variational principle to the integral

$$I = \int \Psi(H-E)\Psi \,\mathrm{d}\tau \tag{12}$$

(Jones 1975). Using nonrelativistic single-configuration HF wavefunctions to describe the target (Froese-Fischer 1972), we obtain

$$\left(\frac{\mathrm{d}^2}{\mathrm{d}r^2}+k^2-\frac{l(l+1)}{r^2}\right)f(r) = -2V(r)f(r)+2W(r)f(r)+2V_{\mathrm{R}}(r)f(r), \tag{13}$$

with $r^{-1}f(r)$ equivalent to $F(r)$ of equation (3b). In equation (13) the static potential $V(r)$ is

$$V(r) = Zr^{-1} - \sum_{n'l'} 2(2l'+1)\,\mathrm{Y}_0(P_{n'l'},P_{n'l'};r), \tag{14}$$

where the $n'l'$ summation is over all closed subshells, $r^{-1}P_{nl}(r)$ is equivalent to $R_{n\kappa}(r)$ of equation (3a) and

$$\mathrm{Y}_\lambda(P_{n'l'},P_{n'l'};r) = r^{-(\lambda+1)}\int_0^r P_{n'l'}(s)\,P_{n'l'}(s)\,s^\lambda\,\mathrm{d}s + r^\lambda\int_r^\infty P_{n'l'}(s)\,P_{n'l'}(s)\,s^{-(\lambda+1)}\,\mathrm{d}s. \tag{15}$$

The exchange term in equation (13) is given by

$$W(r)f(r) = -\sum_{n'l'}\sum_\lambda \frac{2l'+1}{2l+1}(\mathrm{C}^{l'\lambda l}_{000})^2\,\mathrm{Y}_\lambda(P_{n'l'},f;r)\,P_{n'l'}(r), \tag{16}$$

where the $n'l'$ summation is again over all closed subshells. Following Hartree (1957), the functions $\mathrm{Y}_\lambda(P,f;r)$ satisfy the second-order differential equation

$$\mathrm{d}^2(r\mathrm{Y}_\lambda)/\mathrm{d}r^2 = \lambda(\lambda+1)r^{-2}(r\mathrm{Y}_\lambda) - (2\lambda+1)r^{-1}P(r)f(r), \tag{17}$$

with the boundary conditions

$$rY_\lambda(r) \sim r^{\lambda+1} \quad \text{as} \quad r \to 0, \tag{18a}$$

$$\sim r^{-\lambda} \quad\quad r \to \infty. \tag{18b}$$

Note that equations (14)–(16) would not be valid if relativistic wavefunctions were used to describe the target.

The relativistic correction V_R to the potential of equation (13) is derived using equations (1)–(4) and (10) and (11) with the relation

$$\boldsymbol{l}.\boldsymbol{s}.\chi_{\kappa\mu} = \tfrac{1}{2}\{\boldsymbol{J}^2-\boldsymbol{L}^2-\boldsymbol{S}^2\}\chi_{\kappa\mu} = \tfrac{1}{2}\{j(j+1)-l(l+1)-\tfrac{3}{4}\}\chi_{\kappa\mu}. \tag{19}$$

We write

$$V_R = v(\mathrm{M}) + v(\mathrm{D}) + v(\mathrm{SO}) \tag{20}$$

where the mass correction is

$$v(\mathrm{M}) = -\tfrac{1}{8}\alpha^2\{k^2+2V(r)\}^2, \tag{21a}$$

the Darwin correction is

$$v(\mathrm{D}) = -\tfrac{1}{8}Z\alpha^2 \sum_{n'l'} \delta_{ll'}\,\delta_{mm'}\,\delta_{l'0}\,R_{n'l'}(0)\,F_l(0) \tag{21b}$$

and the spin–orbit coupling term is

$$v(\mathrm{SO}) = -\tfrac{1}{2}\alpha^2(1+\kappa)\,r^{-1}\{2+\alpha^2V(r)\}^{-2}\,\mathrm{d}V/\mathrm{d}r. \tag{21c}$$

The Darwin correction (21b) is non-vanishing for s-wave scattering only, while the spin–orbit interaction is zero in this case. The potential (21c) which describes the spin–orbit effect has the proper behaviour near the origin (Condon and Shortley 1964; Norcross 1973). Electron exchange effects in the relativistic corrections are neglected here (Jones 1970). These effects can be taken into account by using, instead of the static potential $V(r)$ in equations (20) and (21a, c), a potential of the form

$$V_x(r) = V(r) + 6\{-(3/8\pi)\rho(r)\}^{\frac{1}{3}}, \tag{22}$$

where $\rho(r)$ is the charge density. The last term on the right-hand side of equation (22) is the free electron exchange potential (Slater 1960; Herman and Skillman 1963). For electron–atom scattering, relativistic effects become important near the origin, where the potential is dominated by the Coulomb field. Thus the static potential $V(r)$ can be used here instead of $V_x(r)$, which allows for electron exchange.

(2) *Second-order Dirac Potential*

The Dirac relativistic equation for the continuum function can be written in the form

$$\left(\frac{\mathrm{d}^2}{\mathrm{d}r^2}+\frac{(1+\gamma)k^2}{2}-\frac{l(l+1)}{r^2}\right)G_\kappa(r) = -2\gamma\,V(r)\,G_\kappa(r) - \alpha^2\left(V^2(r) - \frac{\kappa\,V'(r)}{r\{\gamma+1+\alpha^2V(r)\}}\right.$$
$$\left. + \frac{V''(r)}{2\{\gamma+1+\alpha^2V(r)\}} - \frac{3\alpha^2V'^2(r)}{4\{\gamma+1+\alpha^2V(r)\}^2}\right)G_\kappa(r) = 0, \tag{23}$$

if electron exchange is neglected (Mott and Massey 1965; Browne and Bauer 1966).

Here $\gamma = (1-v^2/c^2)^{-\frac{1}{2}}$, with v the electron velocity and c the velocity of light; γ is equal to 1 for low energies. Comparing equations (13) and (23), we choose as another form of relativistic correction to the potential in (13)

$$V_{\mathrm{R}} = -\tfrac{1}{2}\alpha^2\left(V^2(r) - \frac{\kappa\, V'(r)}{r\{\gamma+1+\alpha^2 V(r)\}} + \frac{V''(r)}{2\{\gamma+1+\alpha^2 V(r)\}} - \frac{3\alpha^2 V'^2(r)}{4\{\gamma+1+\alpha^2 V(r)\}^2}\right). \tag{24}$$

The first term on the right-hand side of this equation is the mass correction which is similar to $v(\mathrm{M})$ of equation (21a). The remaining terms describe the spin–orbit interaction and other relativistic effects.

Boundary Conditions near the Origin

We now consider the behaviour of the radial part of the continuum function near the origin for the following cases.

(i) Without relativistic correction, we have

$$f_l(r) \sim r^{l+1} \qquad \text{as} \qquad r \to 0. \tag{25}$$

This is the well-known solution of the nonrelativistic Schrödinger equation near the origin.

(ii) With relativistic correction using the Pauli approximation, we have

$$f_\kappa(r) \sim r^\lambda \qquad \text{as} \qquad r \to 0, \tag{26a}$$

$$\lambda = \tfrac{1}{2} + \{l(l+1) - \alpha^2 Z^2 + \tfrac{1}{4}\}^{\frac{1}{2}}. \tag{26b}$$

The relation (26b) is only valid for $l \neq 0$. With $l = 0$, the potential is dominated by the relativistic correction which is attractive with an r^{-2} singularity near the origin. Such a potential is inadmissible (Rose and Newton 1951).

(iii) With relativistic correction using the second-order Dirac potential, we have

$$f_\kappa(r) \sim r^\lambda \qquad \text{as} \qquad r \to 0, \tag{27a}$$

$$\lambda = \tfrac{1}{2} + (\kappa^2 - \alpha^2 Z^2)^{\frac{1}{2}}. \tag{27b}$$

Here, for a given value of l, the indicial function is not the same for spin up and spin down.

Cross Section and Spin Polarization

In the nonrelativistic problem, the collision is described by the scattering amplitude

$$f(\theta) = \frac{1}{2ik}\sum_{l=0}^{\infty} (2l+1)\{\exp(i2\eta_l) - 1\}\, \mathrm{P}_l(\cos\theta) \tag{28}$$

and the differential cross section is given by

$$I(\theta) = |f(\theta)|^2. \tag{29}$$

In the relativistic case there are two scattering amplitudes,

$$f(\theta) = \frac{1}{2ik}\sum_{l=0}^{\infty}\left[(l+1)\{\exp(\mathrm{i}2\eta_l^{+})-1\} + l\{\exp(\mathrm{i}2\eta_l^{-})-1\}\right]\mathrm{P}_l(\cos\theta), \tag{30a}$$

$$g(\theta) = \frac{1}{2ik}\sum_{l=0}^{\infty}\left[\exp(\mathrm{i}2\eta_l^{-}) - \exp(\mathrm{i}2\eta_l^{+})\right]\mathrm{P}_l^1(\cos\theta), \tag{30b}$$

where $\mathrm{P}_l(\cos\theta)$ and $\mathrm{P}_l^1(\cos\theta)$ are the Legendre and associated Legendre polynomials (Mott 1929), and the plus and minus superscripts denote spin-up and spin-down cases respectively. The differential cross section is

$$I(\theta,\phi) = |f|^2+|g|^2+\left(fg^*-gf^*\right)\left(\frac{-AB^*\exp(\mathrm{i}\phi)+A^*B\exp(-\mathrm{i}\phi)}{|A|^2+|B|^2}\right), \tag{31}$$

where the parameters A and B describe the initial spin state of the incident electron. For an unpolarized incident beam, we have

$$I(\theta) = |f|^2+|g|^2. \tag{32}$$

The spin polarization $P(\theta)$ is written as

$$P(\theta) = \mathrm{i}(fg^*-f^*g)/I(\theta), \tag{33}$$

while the total scattering and momentum transfer cross sections for elastic scattering are defined respectively as

$$\sigma_{\mathrm{T}} = \int I(\theta)\,\mathrm{d}\Omega, \qquad \sigma_{\mathrm{M}} = \int I(\theta)(1-\cos\theta)\,\mathrm{d}\Omega. \tag{34a, b}$$

For the nonrelativistic case, we obtain readily

$$\sigma_{\mathrm{T}} = \frac{4\pi}{k^2}\sum_l (2l+1)\sin^2\eta_l, \qquad \sigma_{\mathrm{M}} = \frac{4\pi}{k^2}\sum_l (l+1)\sin^2(\eta_l-\eta_{l+1}). \tag{35a, b}$$

For the relativistic case, we find using equations (30), (32) and (34)

$$\sigma_{\mathrm{T}} = \frac{4\pi}{k^2}\sum_l \left((l+1)\sin^2\eta_l^{+} + l\sin^2\eta_l^{-}\right), \tag{36a}$$

$$\sigma_{\mathrm{M}} = \frac{4\pi}{k^2}\sum_l\left(\frac{(l+1)(l+2)}{2l+3}\sin^2(\eta_l^{+}-\eta_{l+1}^{+}) + \frac{l(l+1)}{2l+1}\sin^2(\eta_l^{-}-\eta_{l+1}^{-}) + \frac{l+1}{(2l+1)(2l+3)}\sin^2(\eta_l^{+}-\eta_{l+1}^{-})\right). \tag{36b}$$

An outline of the derivation of equation (36b) is given in the Appendix.

Results

The results of the present calculations for s-wave scattering are shown in Fig. 1*a*. It is seen that it is important to allow for electron exchange (curve 2). More than 90% of the contribution to exchange was found to be given by the $n = 5$ and 6

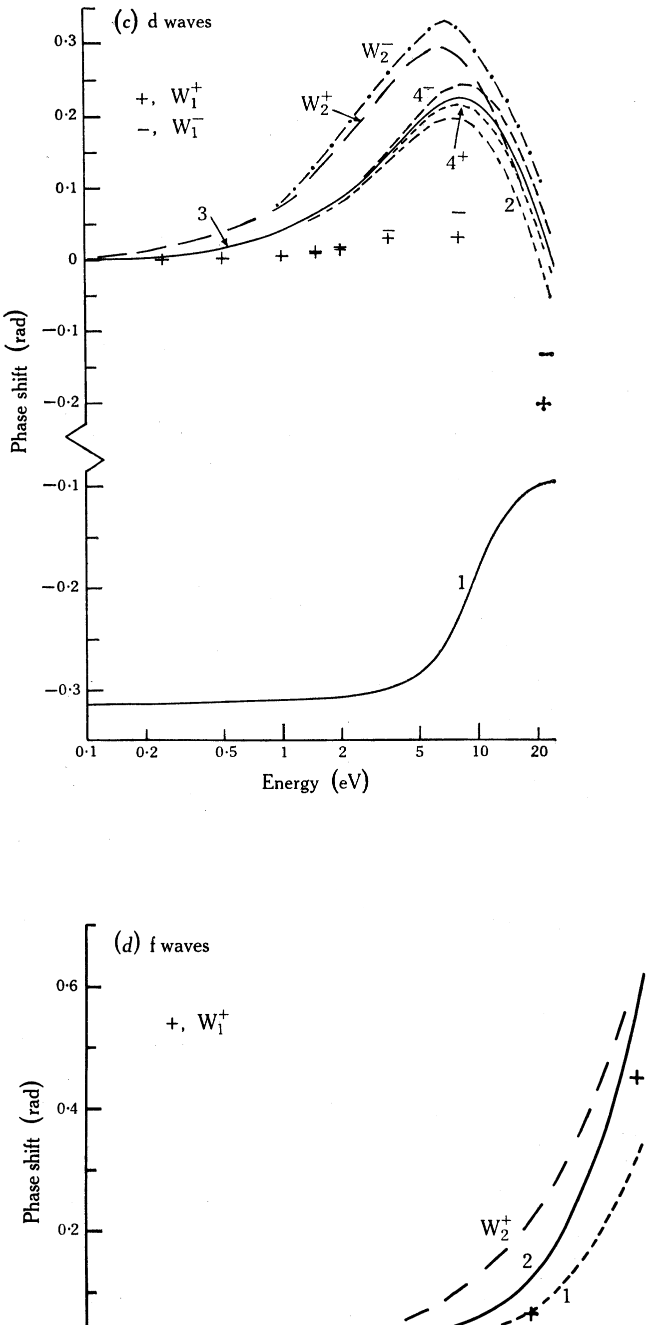

Figs 1*c* and 1*d* [see caption below Fig. 1*a*]

significant contribution (curve 3). The potential becomes more attractive and the phase shift is increased. The inclusion of the spin–orbit correction in the calculation gives two sets of values with spin up and spin down, and the splitting occurs about

The phase shift for spin down is increased since the potential becomes more attractive, and vice versa for spin up. The relativistic correction based on the second-order Dirac potential (curve 4) includes higher order effects and therefore causes a larger splitting between the $p_{1/2}$ and $p_{3/2}$ partial wave phase shifts than that due to the correction based on the Pauli approximation (curve 5).

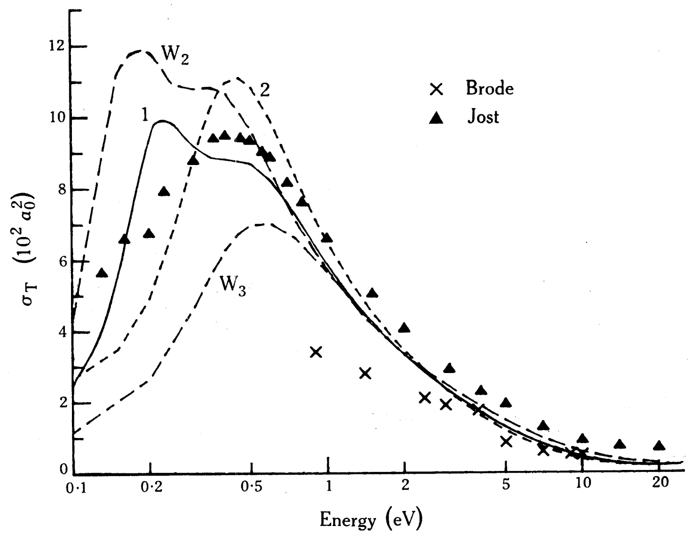

Fig. 2. Comparison of theoretical results for the total scattering cross section σ_T for electrons in mercury with the experimental data of Brode (1929) and Jost and Ohnemus (1979): 1, 2, present results using the second-order Dirac potential and the Pauli approximation respectively; W_2, W_3, Walker (1975, personal communication) relativistic exchange and polarization by POM and PPP analyses respectively.

The calculation for p-wave scattering indicates also the presence of a broad shape resonance at low energy. Consequently, the calculated phase shift is very sensitive to the potential used. There are two resonance peaks: an extremely broad one due to the $p_{3/2}$ partial wave and a much sharper one due to the $p_{1/2}$ partial wave, at an energy of $\sim 0 \cdot 25$ eV with the second-order Dirac potential and at $\sim 0 \cdot 35$ eV with the Pauli approximation. The present phase shifts are larger than the exchange results (W_1) of Walker (1969), who solved the Dirac equation explicitly (Fig. $1b_2$). The discrepancy may be due to the use of the nonrelativistic HF wavefunction for the target in the present work, whereas single-configuration relativistic orbitals were used by Walker. To obtain the low energy resonance, Walker (1975) included polarization using the POM analysis and found the position of the $p_{1/2}$ wave resonance to be at an energy of $\sim 0 \cdot 2$ eV (W_2 results in Fig. $1b_3$).

The results for d-wave and f-wave scattering are shown in Figs 1*c* and 1*d* respectively. Relativistic effects are small for d wave and negligible for f wave. The splitting between the $d_{5/2}$ and $d_{3/2}$ partial wave phase shifts due to the relativistic correction based on the Pauli approximation is smaller than that based on the second-order Dirac potential. The results obtained with the Pauli approximation are not shown in Fig. 1*c*. Only the $n = 5$ and 6 orbitals were used when calculating exchange for f-wave scattering.

The total cross section σ_T predicted by theory is compared in Fig. 2 with the measurements of Brode (1929) and Jost and Ohnemus (1979). The presence of a low energy resonance at $\sim 0\cdot 63$ eV was first reported by Burrow and Michejda (1975). In the recent experiment of Jost and Ohnemus, the position of the resonance was observed to be $\sim 0\cdot 4$ eV. Two sets of total cross sections have been calculated, based on the second-order Dirac potential and the Pauli approximation, with partial wave phase shifts for $l = 0$–10. Exchange was neglected in calculating the phase shift for partial waves with $l > 4$, while the exchange s-wave phase shift was used in the calculation of the total cross section in the Pauli approximation. (The same procedure was adopted in the calculation of the momentum transfer cross section, the differential cross section and the spin polarization; Figs 3, 4 and 5 below.)

Table 1. Contributions of $p_{1/2}$ and $p_{3/2}$ partial waves to the total cross section in the energy region of the resonance

The results for the total scattering cross section σ_T calculated by the two theoretical methods are shown. All cross section values are in units of a_0^2

Energy	Second-order Dirac potential			Pauli approximation		
(eV)	$\sigma_T(p_{1/2})$	$\sigma_T(p_{3/2})$	$\sigma_T(p_{1/2})+\sigma_T(p_{3/2})$	$\sigma_T(p_{1/2})$	$\sigma_T(p_{3/2})$	$\sigma_T(p_{1/2})+\sigma_T(p_{3/2})$
0·1	101·09	20·88	121·97	25·02	25·61	50·63
0·15	369·12	52·18	421·30	70·83	65·65	136·48
0·2	698·99	101·28	800·27	152·06	130·45	282·51
0·25	683·56	168·33	851·19	260·35	220·03	480·38
0·3	537·90	248·30	786·20	356·75	324·33	681·08
0·35	424·69	330·08	754·77	403·02	424·63	827·65
0·4	349·35	401·20	750·55	401·66	501·94	903·60
0·5	261·19	481·63	742·82	341·77	559·73	901·50
0·6	212·91	486·37	699·28	281·08	532·05	813·13
0·7	182·60	454·66	637·26	236·25	478·25	714·50
0·8	161·67	413·45	575·12	203·89	425·20	629·09
0·9	146·18	373·96	520·14	179·87	379·58	559·45
1·0	134·12	339·21	473·33	161·48	341·80	503·28
1·5	98·27	227·45	325·72	109·65	227·72	337·37
2·0	78·81	169·82	248·63	84·18	170·82	255·00

Fig. 2 also shows the results (W_2) for the total cross section obtained by Walker (1975), with polarization taken into account by a POM analysis. In a more recent calculation, Walker (personal communication) has used a pseudo-polarization potential (PPP) with a cutoff parameter chosen to give a best fit to the resonance observed by Elford (1980). The results of these calculations are also included for comparison in Fig. 2 (W_3 curve).

It is of interest to analyse the configuration of the resonance observed experimentally. Table 1 lists the contributions of the $p_{1/2}$ and $p_{3/2}$ partial waves to the total cross section in the energy region of the resonance. It is seen that there is a large contribution from both partial waves. The $p_{3/2}$ resonance is broad and lies at a higher energy than the $p_{1/2}$ resonance (Fig. $1b_2$), but the spin-up case has a greater weight than the spin-down one (see equation 36a). The present calculation indicates that the structure observed by Burrow and Michejda (1975) and others seems to be most likely a mixture of the $p_{1/2}$ and $p_{3/2}$ resonances with the configurations $(6s^2\,6p_{1/2})\,^2P_{1/2}$ and $(6s^2\,6p_{3/2})\,^2P_{3/2}$ respectively.

Fig. 3 compares the present calculated results for the momentum transfer cross section σ_M with the experimental data of Nakamura and Lucas (1978) and Elford (1980). The results of Rockwood (1973), derived from the experimental data of McCutchen (1958), are also included. In the swarm experiment by Elford, a low energy resonance was observed at $\sim 0 \cdot 5$ eV. As can be seen from Fig. 3, there is agreement between theory and experiment at energies above this resonance position, but the calculations are much larger at low energies.

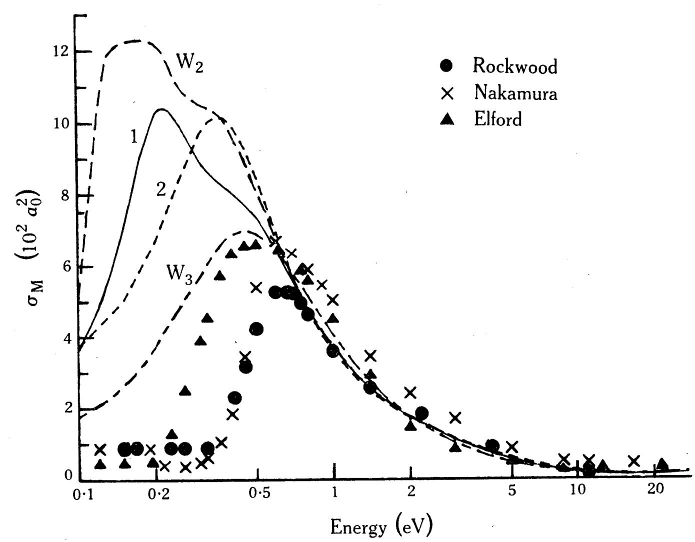

Fig. 3. Comparison of theoretical results for the momentum transfer cross section σ_M for electrons in mercury with the experimental data of Rockwood (1973), Nakamura and Lucas (1978) and Elford (1980): 1, 2, present results using the second-order Dirac potential and the Pauli approximation respectively; W_2, W_3, Walker (1975, personal communication) relativistic exchange and polarization by POM and PPP analyses respectively.

The results for the differential cross sections $I(\theta)$ at energies of 1·4, 2·4, 3·9, 7 and 25 eV are presented in Fig. 4, where they are compared with the experimental data of Duweka *et al.* (1976) at the three lowest energies, Deichsel *et al.* (1966) at 7 eV and Eitel and Kessler (1970) at 25 eV. The mean values of the experimental cross sections for scattering to the right and left are normalized at 55° to the present calculation based on the second-order Dirac potential. The W_2 calculation by Walker (1975) is also included; his results at 3·5 eV are shown in Fig. 4*c*.

Finally, Fig. 5 shows the results for the spin polarization $P(\theta)$ at the same energies as in Fig. 4. Again included for comparison are the measurements of Duweka *et al.* (1976), Deichsel *et al.* (1966) and Eitel and Kessler (1970), together with the W_2 calculations by Walker (1975). The present calculation based on the second-order Dirac potential (curve 1) seems to give better agreement with experiment. In particular, the calculation based on the Pauli approximation (curve 2) fails to reproduce the qualitative features of the measurement at 25 eV. This may be due to the use of the s-wave phase shift with exchange only when calculating the spin polarization based on the Pauli approximation.

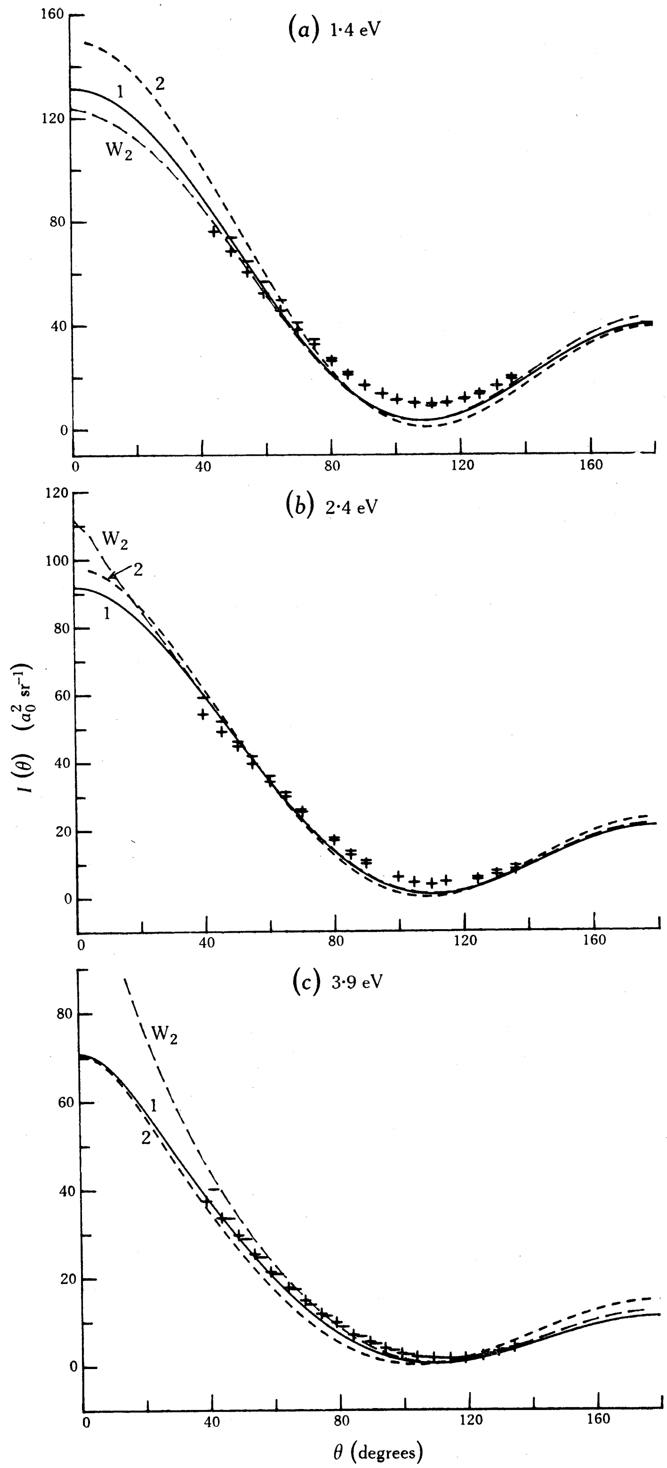

Figs 4*a*–4*c* [see caption on facing page]

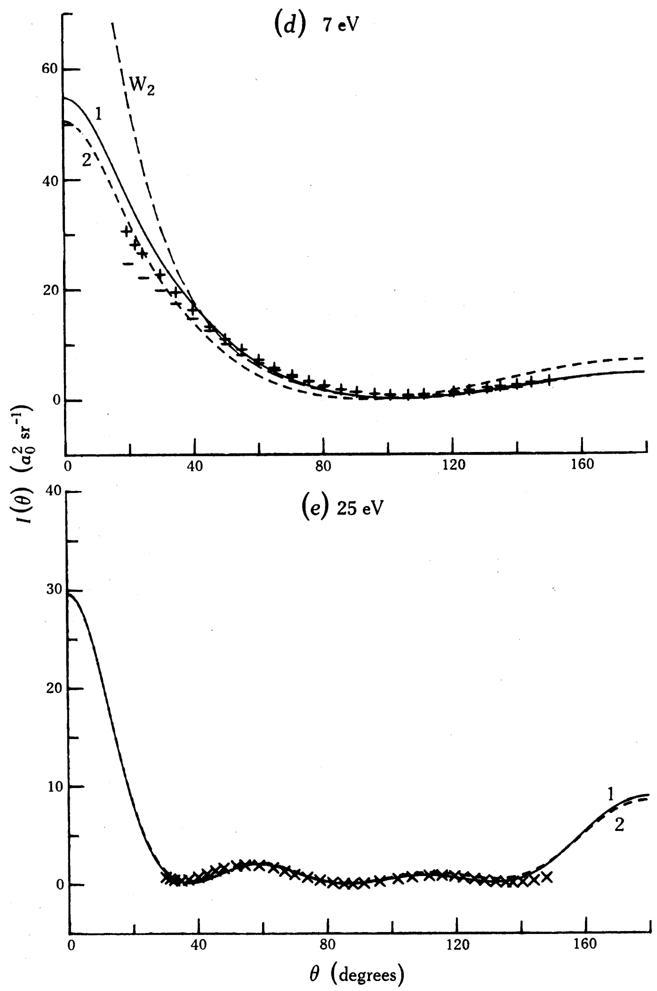

Figs 4*a*–4*e*. Comparison of theoretical and experimental results for the differential cross section $I(\theta)$ for electrons in mercury at the indicated energies. The theoretical curves are: 1, 2, present results using the second-order Dirac potential and the Pauli approximation respectively; W_2, Walker (1975) relativistic exchange and polarization by POM analysis (his results at 3·5 eV are shown in (*c*)). The experimental data of (*a*,*b*,*c*) Duweka *et al.* (1976) and (*d*) Deichsel *et al.* (1966) are plotted as plus and minus signs for scattering to the right and left respectively, the mean values being normalized to the present calculation 1 at a scattering angle θ of 55°. Similarly the experimental data of Eitel and Kessler (1970), plotted as crosses in (*e*), have been normalized to the present calculation 1 at $\theta = 55°$.

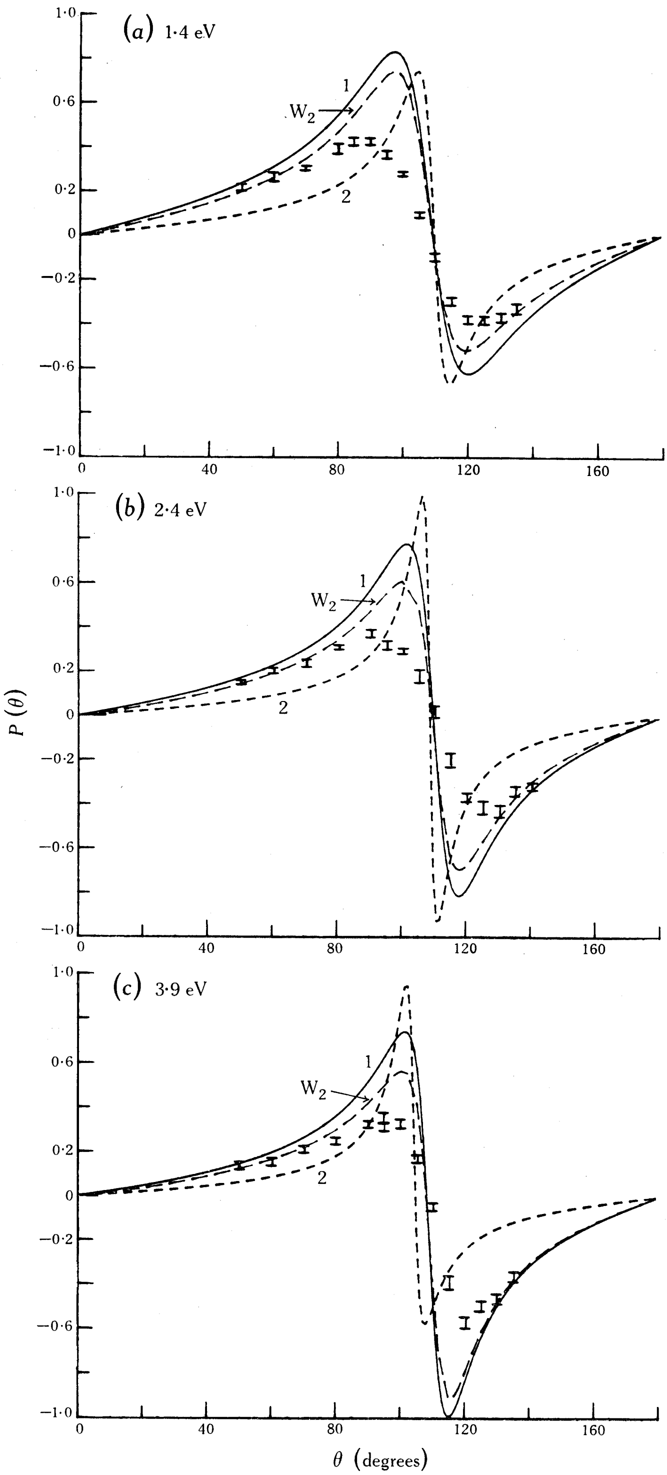

Figs 5*a*–5*c* [see caption on facing page]

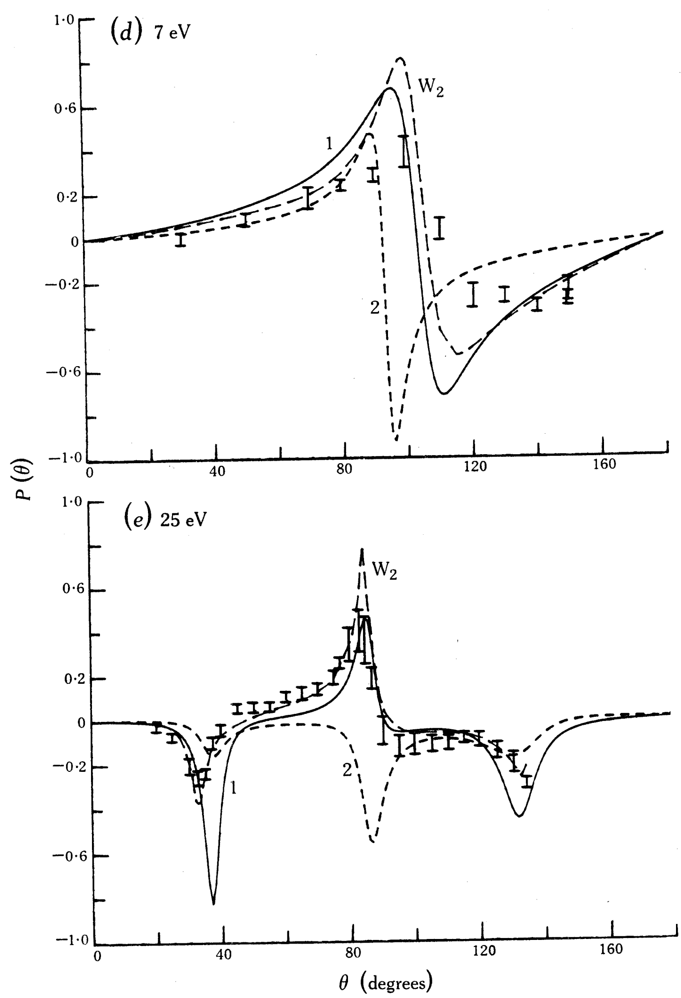

Figs 5*a*–5*e*. Comparison of theoretical and experimental results for the spin polarization $P(\theta)$ for electrons in mercury at the indicated energies. The theoretical curves are: 1, 2, present results using the second-order Dirac potential and the Pauli approximation respectively; W_2, Walker (1975) relativistic exchange and polarization by POM analysis (his results at 3·5 eV are shown in (*c*)). The plotted experimental data are from (*a,b,c*) Duweka *et al.* (1976), (*d*) Deichsel *et al.* (1966) and (*e*) Eitel and Kessler (1970).

Conclusions

The scattering of low energy electrons by mercury atoms has been investigated using a perturbation method, and relativistic effects have been taken into account using two models: a Pauli approximation and a second-order Dirac potential. We have seen that the relativistic effect due to mass variation makes a significant contribution, in particular for p-wave scattering. The second-order Dirac potential allows for higher order relativistic effects and gives a larger correction to the potential.

There is agreement between the present theory and experiment for the total cross section, momentum transfer cross section, differential cross section and spin polarization at energies above the resonance position. However, the theory predicts a momentum transfer cross section that is larger than experiment at lower energies.

The present calculation indicates features which need further investigation. In particular, the use of the nonrelativistic HF wavefunction to describe the target should be re-examined since it appears that a relativistic wavefunction is required. Also, it may be necessary to allow for the polarization of the target electrons of the systems by the free electron as well as for the core polarization of the target (Baylis 1977). These features will be considered in a future report.

Acknowledgments

The author is grateful to Dr M. Elford for suggesting and encouraging this project, and for making available his experimental results prior to publication. He wishes to thank Dr R. W. Crompton, Dr T. F. O'Malley and Professor K. Nygaard for many discussions, Dr D. Walker for making available theoretical results beyond those published, Professor C. Froese-Fischer and Professor W. Baylis for useful correspondence and Dr R. O. Watts for his encouragement and interest in the work.

References

Baylis, W. E. (1977). *J. Phys.* B **10**, L583–7.
Beck, D. R. (1969). *J. Chem. Phys.* **51**, 2171–83.
Bethe, H. A., and Salpeter, E. E. (1957). 'Quantum Mechanics of One- and Two-electron Atoms' (Springer: Berlin).
Blume, M., and Watson, R. E. (1962). *Proc. R. Soc. London* A **270**, 127–43.
Blume, M., and Watson, R. E. (1963). *Proc. R. Soc. London* A **271**, 565–78.
Blume, M., and Watson, R. E. (1964). *Phys. Rev.* **34**, A320–7.
Bransden, B. H. (1976). *In* 'Electron and Photon Interaction with Atoms' (Eds H. Kleinpoppen and M. R. C. McDowell) (Plenum: New York).
Brode, R. B. (1929). *Proc. R. Soc. London* A **125**, 134–42.
Browne, H. N., and Bauer, E. (1966). *Phys. Rev. Lett.* **16**, 495–8.
Bühring, W. (1968). *Z. Phys.* **212**, 61–70.
Bunyan, P. J. (1963). *Proc. Phys. Soc. London* **81**, 816–19.
Burke, P. G., and Mitchell, J. F. B. (1974). *J. Phys.* B **2**, 214–28.
Burrow, P. D., and Michejda, J. A. (1975). *Bull. Am. Phys. Soc.* **20**, 252–3.
Carse, G. D., and Walker, D. W. (1973). *J. Phys.* B **6**, 2529–44.
Condon, E. U., and Shortley, G. H. (1964). 'The Theory of Atomic Spectra' (Cambridge Univ. Press).
Coulthard, M. A. (1967). *Proc. Phys. Soc. London* **91**, 44–9.
Deichsel, H. E., Reichert, E., and Steidl, H. (1966). *Z. Phys.* **189**, 212–16.
Desclaux, J. P., Mayers, D. F., and O'Brien, F. (1971). *J. Phys.* B **4**, 631–42.
Duweka, M., Kirchner, N., Reichert, E., and Schön, S. (1976). *J. Phys.* B **9**, 1915–21.
Eitel, W., Jost, W., and Kessler, J. (1968). *Z. Naturf.* (a) **23**, 2122–3.
Eitel, W., and Kessler, J. (1970). *Phys. Rev. Lett.* **24**, 1472–3.
Elford, M. T. (1980). *Aust. J. Phys.* **33**, 251–9.
Froese-Fischer, C. (1972). *At. Data* **4**, 301–99.
Grant, I. P. (1961). *Proc. R. Soc. London* A **262**, 555–76.
Hartree, D. R. (1957). 'The Calculation of Atomic Structures' (Wiley: New York).
Herman, F., and Skillman, S. (1963). 'Atomic Structure Calculations' (Prentice-Hall, Englewood Cliffs, N.J.).
Holzwarth, G., and Meister, H. J. (1964). *Nucl. Phys.* **59**, 56–64.

Hutt, P. K. (1975). *J. Phys.* B **8**, L88–91.
Hutt, P. K., and Bransden, B. H. (1974). *J. Phys.* B **7**, 2223–9.
Jones, M. (1970). *J. Phys.* B **3**, 1571–92.
Jones, M. (1975). *Phil. Trans. R. Soc. London* A **277**, 587–622.
Jost, K., and Ohnemus, B. (1979). *Phys. Rev.* A **19**, 641–54.
Kessler, J. (1969). *Rev. Mod. Phys.* **41**, 3–25.
Kim, Y. K. (1967). *Phys. Rev.* **154**, 17–39.
McCutchen, C. W. (1958). *Phys. Rev.* **112**, 1848–51.
Malli, G. (1967). *J. Chem. Phys.* **47**, 2217–19.
Morse, P. M., and Feshbach, H. (1953). 'Methods of Theoretical Physics', Vol. 1 (McGraw-Hill: New York).
Mott, N. F. (1929). *Proc. R. Soc. London* A **124**, 425–42.
Mott, N. F., and Massey, H. W. S. (1965). 'The Theory of Atomic Collisions' (Oxford Univ. Press).
Nakamura, Y., and Lucas, J. (1978). *J. Phys.* D **11**, 336–45.
Norcross, D. W. (1973). *Phys. Rev.* A **7**, 606–16.
Rockwood, S. D. (1973). *Phys. Rev.* A **8**, 2348–58.
Rose, M. E., and Newton, R. R. (1951). *Phys. Rev.* **82**, 470–7.
Slater, J. C. (1960). 'Quantum Theory of Atomic Structure', Vol. 1 (McGraw-Hill: New York).
Swirles, B. (1935). *Proc. R. Soc. London* A **152**, 625–49.
Walker, D. W. (1969). *J. Phys.* B **2**, 356–66.
Walker, D. W. (1970*a*). *J. Phys.* B **3**, 788–97.
Walker, D. W. (1970*b*). *J. Phys.* B **3**, L123–5.
Walker, D. W. (1971). *Adv. Phys.* **20**, 257–323.
Walker, D. W. (1975). *J. Phys.* B **8**, L161–3.
Weiss, H. F. (1969). *Z. Phys.* **229**, 299–308.

Appendix

From equations (30) we have

$$\begin{aligned}|f(\theta)|^2 = \frac{1}{k^2}\sum_{l,l'} [&(l+1)(l'+1)\sin\eta_l^+ \sin\eta_{l'}^+ \cos(\eta_l^+ - \eta_{l'}^+) \\ &+ ll' \sin\eta_l^- \sin\eta_{l'}^- \cos(\eta_l^- - \eta_{l'}^-) + (l+1)l' \sin\eta_l^+ \sin\eta_{l'}^- \cos(\eta_l^+ - \eta_{l'}^-) \\ &+ l(l'+1)\sin\eta_l^- \sin\eta_{l'}^+ \cos(\eta_l^- - \eta_{l'}^+)]\, \mathrm{P}_l(\cos\theta)\,\mathrm{P}_{l'}(\cos\theta)\,, \end{aligned} \tag{A1a}$$

$$\begin{aligned}|g(\theta)|^2 = \frac{1}{2k^2}\sum_{l,l'} [&-\sin^2(\eta_l^+ - \eta_{l'}^+) + \sin^2(\eta_l^- - \eta_{l'}^+) \\ &+ \sin^2(\eta_l^+ - \eta_{l'}^-) - \sin^2(\eta_l^- - \eta_{l'}^-)]\, \mathrm{P}_l^1(\cos\theta)\,\mathrm{P}_{l'}^1(\cos\theta)\,. \end{aligned} \tag{A1b}$$

Then, using the relations

$$(2l+1)z\,\mathrm{P}_l^m(z) = (l-m+1)\,\mathrm{P}_{l+1}^m(z) + (l+m)\,\mathrm{P}_{l-1}^m(z)\,, \tag{A2a}$$

$$\int_{-1}^{+1} \mathrm{P}_l^m(z)\,\mathrm{P}_{l'}^m(z)\,\mathrm{d}z = \frac{2}{2l+1}\frac{(l+m)!}{(l-m)!}\delta_{ll'} \tag{A2b}$$

(Morse and Feshbach 1953), we obtain

$$\int |f(\theta)|^2(1-\cos\theta)\,\mathrm{d}\Omega$$

$$= \frac{4\pi}{k^2}\sum_l\left\{\frac{(l+1)^2}{(2l+1)(2l+3)}\left(-\sin^2\eta_l^+ + 2(l+2)\sin\eta_l^+\cos\eta_{l+1}^+\sin(\eta_l^+-\eta_{l+1}^+)\right)\right.$$

$$+\frac{l}{(2l+1)(2l+3)}\left(-(l+2)\sin^2\eta_l^- + 2(l+1)^2\sin\eta_l^-\cos\eta_{l+1}^-\sin(\eta_l^- - \eta_{l+1}^-)\right)$$

$$-\frac{2(l+1)^3}{(2l+1)(2l+3)}\sin\eta_l^+\sin\eta_{l+1}^-\cos(\eta_l^+-\eta_{l+1}^-)$$

$$-\frac{2l(l+1)(l+2)}{(2l+1)(2l+3)}\sin\eta_l^-\sin\eta_{l+1}^+\cos(\eta_l^- - \eta_{l+1}^+)$$

$$\left.+\frac{2l(l+1)}{2l+1}\sin\eta_l^+\sin\eta_l^-\cos(\eta_l^+-\eta_l^-)\right\}, \tag{A3a}$$

$$\int |g(\theta)|^2(1-\cos\theta)\,\mathrm{d}\Omega$$

$$= \frac{4\pi}{k^2}\sum_l\left\{\frac{l(l+1)}{2l+1}\sin^2(\eta_l^+-\eta_l^-) + \frac{l(l+1)(l+2)}{(2l+1)(2l+3)}\sin^2(\eta_l^+-\eta_{l+1}^+)\right.$$

$$+\frac{l(l+1)(l+2)}{(2l+1)(2l+3)}\sin^2(\eta_l^- - \eta_{l+1}^-) - \frac{l(l+1)(l+2)}{(2l+1)(2l+3)}\sin^2(\eta_l^+-\eta_{l+1}^-)$$

$$\left.-\frac{l(l+1)(l+2)}{(2l+1)(2l+3)}\sin^2(\eta_l^- - \eta_{l+1}^+)\right\}. \tag{A3b}$$

To derive the momentum transfer cross section defined by

$$\sigma_{\mathrm{M}} = \int \{|f(\theta)|^2 + |g(\theta)|^2\}(1-\cos\theta)\,\mathrm{d}\Omega, \tag{A4}$$

consider first, for example, the sum S of the third and fourth terms on the right-hand sides of equations (A3a) and (A3b):

$$S \equiv -\frac{4\pi}{k^2}\sum_l\frac{l+1}{(2l+1)(2l+3)}\left(2(l+1)^2\sin\eta_l^+\sin\eta_{l+1}^-\cos(\eta_l^+-\eta_{l+1}^-)\right.$$

$$\left.+l(l+2)\sin^2(\eta_l^+-\eta_{l+1}^-)\right)$$

$$= -\frac{4\pi}{k^2}\sum_l\frac{l+1}{(2l+1)(2l+3)}\left(-\sin^2(\eta_l^+-\eta_{l+1}^-) + (l+1)^2\{\sin^2(\eta_l^+-\eta_{l+1}^-)\right.$$

$$\left.+2\sin\eta_l^+\sin\eta_{l+1}^-\cos(\eta_l^+-\eta_{l+1}^-)\}\right)$$

$$= -\frac{4\pi}{k^2}\sum_l\frac{l+1}{(2l+1)(2l+3)}\left(-\sin^2(\eta_l^+-\eta_{l+1}^-) + (l+1)^2[1-\cos(\eta_l^+-\eta_{l+1}^-)\right.$$

$$\left.\times\{\cos(\eta_l^+-\eta_{l+1}^-) - 2\sin\eta_l^+\sin\eta_{l+1}^-\}]\right). \tag{A5}$$

Using the identities

$$2\cos\alpha\cos\beta = \cos(\alpha-\beta)+\cos(\alpha+\beta), \qquad 2\sin\alpha\sin\beta = \cos(\alpha-\beta)-\cos(\alpha+\beta), \tag{A6}$$

we can reduce equation (A5) to

$$S = \frac{4\pi}{k^2}\sum_l \frac{l+1}{(2l+1)(2l+3)}\Big(\sin^2(\eta_l^+ - \eta_{l+1}^-) - (l+1)^2(\sin^2\eta_l^+ + \sin^2\eta_{l+1}^-)\Big). \tag{A7}$$

The above procedure is applied to simplify the sum of equations (A3a) and (A3b) and, after further algebraic manipulation, the result is the analytical expression for σ_{M} given by equation (36b).

Manuscript received 23 July 1979, accepted 21 September 1979